VSP

Advanced Composite Materials 20 (2011) 547–567

ADVANCED COMPOSITE MATERIALS
brill.nl/acm

Flexural Behavior of Full-Scale Composite Structural Insulated Floor Panels

Mohammed A. Mousa [a,b] **and Nasim Uddin** [a,*]

[a] Department of Civil, Construction and Environmental Engineering, University of Alabama at Birmingham, 1075 13th Street South, Birmingham, AL 35294-4440, PH 205-934-8432, USA
[b] Department of Civil Engineering, Faculty of Engineering at Shoubra, Benha University, Cairo, Egypt

Received 1 June 2010; accepted 17 August 2011

Abstract
Panelized systems are prefabricated components that are brought to a construction site and assembled into the finished structure. Traditional constructions are often subjected to termite attack, mold buildups and have poor penetration resistance against wind-borne debris. To overcome these problems, a new type of composite structural insulated panel (CSIP) was developed and is analyzed in this study for structural floor applications. The concept of the panel is based on the theory of sandwich construction. The proposed composite panel is made of low cost orthotropic thermoplastic glass/polypropylene (glass–PP) laminate as a facesheet and expanded polystyrene foam (EPS) as a core. Full scale experimental testing was conducted to study the flexural behavior of the CSIP floor member. CSIP floor panels failed due to facesheet/core debonding. Analytical modeling was further presented to predict the interfacial tensile stress at the core/facesheet interface, critical wrinkling stress, flexural strength and deflections for structural CSIP floor panels. The experimental results were validated using the proposed models and were in good agreement.

Keywords
Panelized construction, sandwich composite panels, flexural testing, thermoplastic composites

Nomenclature

b panel width

t_f thickness of FRP facesheet

L panel length

* To whom correspondence should be addressed. E-mail: nuddin@uab.edu
Edited by the JSCM

DOI:10.1163/156855111X610208

c core thickness

d thickness of sandwich panel

l natural half-wavelength of the debonded part

w_{m} out-of-plane displacement of the debonded part

σ_z interfacial tensile stress

E_{c} core modulus of elasticity

D panel flexural rigidity

U panel shear rigidity

P total load applied to the panel

ε_{f} strain in FRP facesheet

ε_{r} rupture strain of the facesheet

E_{f} flexural modulus of glass–PP facesheets

G core shear modulus

M_{n} nominal flexural strength of the panel

1. Introduction

Panelized construction is a method where the building is subdivided into basic planar elements that are typically constructed under some form of mass production then shipped directly to the construction site and assembled into the finished structure. There are many advantages for panelizing structures, including cost reductions, possible through mass production, ease of assembly, a lower skill set required for field construction, quality control and worker safety. Most of the existing panelized products are traditional 'wood-based' structures.

Traditional structural insulated panels (SIPs) are made of foam core sandwiched between sheets of oriented strand board (OSB). Traditional SIPs have demonstrated the capabilities for energy efficient, and affordable housing. However, they are often subjected to termite attack, mold buildups as they subjected to harmful weather conditions, and also have poor penetration resistance against wind-borne debris in the event of hurricanes, windstorms or tornados. To overcome these problems, this paper presents a new composite structural insulated panel (CSIP) to replace the traditional SIPs. CSIPs are made of low cost orthotropic thermoplastic glass/polypropylene (glass–PP) laminate as facesheets and expanded polystyrene foam (EPS) as a core. The concept of the CSIP is based on that of the sandwich structure in which a soft lightweight thicker core is sandwiched between two panels of two strong, thin facing. The facesheets carry the bending stresses while the core resists the shear loads and stabilizes the faces against bulking or wrinkling [1].

The core also increases the stiffness of the structure by holding the facesheets apart. Core materials normally have lower mechanical properties compared to those of facesheets.

Several investigations have been conducted by the authors and others on developing composites panels for building applications using rigid and soft cores with thermoset and thermoplastic facesheets [2–8]. It was demonstrated by these studies that the developed panels can provide much higher strength, stiffness and creep resistance than traditional ones that are made with wood-based facing. Despite the high strength that is provided by these panels, the strength is not the only criterion governing the design of the panel; the deflection and debonding are other aspects that control the design of CSIPs [2]. The developed CSIPs have a very high facesheet/core moduli ratio ($E_f/E_c = 12\,500$) compared with the ordinary sandwich construction in which the ratio is normally limited to 1000 [1]. Further, CSIPs are characterized by low cost, high strength to weight ratio, and lower skill required for field construction, etc. These panels can be used for different elements in the structure, including structural elements (e.g., floors, roofs and load bearing walls) and non-structural elements (e.g., non-load bearing walls, lintels and partitions).

A large number of theoretical and experimental studies have been conducted on sandwich construction to investigate their behavior under different types of loadings including in-plane and out-plane loadings. A general review of failure modes of composites sandwich beams construction was given by Daniel *et al.* [9] while those of sandwich wall were given by Gdoutos *et al.* [10]. Failure modes for sandwich beams include yielding of facesheet in tension, core shear failure and local buckling of facesheet in compression, which is known as 'wrinkling' of facesheets. Failure modes of sandwich wall include global buckling, local buckling, wrinkling and core failure.

In the case of global buckling, the core may exhibit a substantial shearing deformation whereas in case of local buckling the core acts as an elastic foundation for the facesheets in compression [11, 12]. It can take the form of outward or downward. If the local buckling is outward, it is known as debonding; if it is downward, it is known as core crushing. The former occurs in the case of sandwich panel with closed cell cores (e.g., EPS foam) while the latter normally happens in the case of sandwich panels with open cell cores (e.g., honeycomb core) [13]. Among the first to study the behavior of sandwich panels were Gough *et al.* [14] and Hoff and Mautner [15]. They tested sandwich specimens under compressive loading and observed that the general mode of failure was facesheet wrinkling. They also developed formulas to predict the stress in the facesheet at wrinkling. These formulas were then modified to fit the experimental results. The results showed that the wrinkling stress is independent of loading and boundary condition and mainly depends on the facesheets and core moduli. The main objectives of this study are to investigate the flexural behavior of full scale CSIP floor member and to develop models for calculating stresses at debonding, flexural strength and deflection.

2. Research Significance and Practice Applications

The overall goal of this research work is to pioneer a new technology for the development of pre-engineered and prefabricated multifunctional building components that possess improved structural performance, greater durability, higher energy absorption, have a short processing time, and could be installed quickly with limited skilled labor. Traditional SIPs possess a few of these advantages, but there are some problems associated with SIPs. One of the major concerns with the traditional OSB SIPs is the poor impact resistance and tendency to mold buildups, and then rotting, that result in the loss of millions of dollars.

To meet the challenges of high strength and low weight materials, structural composite materials may be suitable candidates. Composite materials have been used in construction for many years because they possess high strength and low weight advantages. Thermoplastic (TP) polymers offer advantages in terms of short processing time, extended shelf life and low-cost raw material. TPs also possess the advantages of high toughness, superior impact property, and ease of reshaping and recycling over thermoset polymer composites. Structural composite materials are flexible and can form irregular shapes, varying sections or detail features. This allows more design flexibility than other traditional construction materials. These benefits of TP based composites have already benefited the construction industry.

This research proposes glass–PP composite structural panels for panelized construction. The sandwich panels that are proposed in this research are described as composite structural insulated panels (CSIPs). These panels can be used for walls, floors and roofs members. However, this study focuses on floor applications. The expected contributions for this research work will be, for the first time ever, the consideration of using prefabricated and low cost CSIPs not only for replacing the destroyed traditional construction, but also for new constructions. The results include analytical tools and design aids for the proposed CSIPs for floor panels. Other impacts of the research include transfer of advanced technology from the material science to the civil engineering field and engaging the composites industry in the construction market.

3. Materials and Manufacturing

The CSIPs that are developed and evaluated in this study are made of low cost thermoplastic glass/polypropylene (glass–PP) laminate as a facesheet and expanded polystyrene foam (EPS) as a core (Fig. 1).

Thermoplastic laminates consist of 70% bi-directional E-glass fibers impregnated with polypropylene (PP) resin. They are produced using a hot-melt impregnation process, also called a DRIFT process [16]. Glass–PP composite sheets were directly obtained from the manufacturer [17]. The mechanical properties of glass–PP composites used in this research, as provided by the manufacturer, are listed in Table 1.

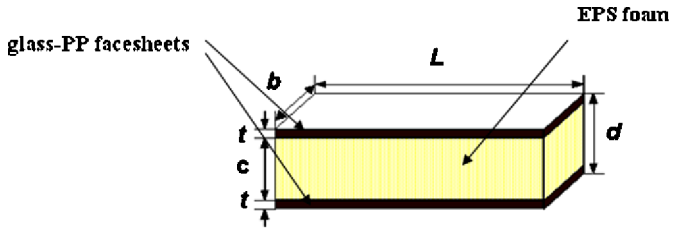

Figure 1. Schematic diagram for the proposed CSIPs floor. This figure is published in color in the online version.

Table 1.
Properties of the glass-PP facesheets

Nominal thickness, t	0.12 in. (3.04 mm)
Weight % of glass fiber	70%
Density (ρ_f)	61 pcf (980 kg/m^3)
Longitudinal modulus (E_x)	2 200 000 psi (15 169 MPa)
Transverse modulus (E_y)	2 200 000 psi (15 169 MPa)
Flexural modulus	2 000 000 psi (13 790 MPa)
Tensile strength	46 000 psi (317 MPa)
Flexural strength	60 000 psi (414 MPa)
In plane-Poisson's ratio (υ_{xy})	0.11

Table 2.
Properties of the EPS foam core

Nominal thickness, c	5.5 in. (140 mm)
Density (ρ_c)	1 pcf (16 kg/m^3)
Elastic modulus (E_c)	180–220 psi (1.2–1.5 MPa)
Flexural strength	25–30 psi (0.1–0.2 MPa)
Shear modulus (G_c)	280–320 psi (1.9–2.2 MPa)
Shear strength	18–22 psi (0.1–0.15 MPa)
Tensile strength	16–20 psi (0.11–0.14 MPa)
Compressive strength	10–14 psi (0.07–0.1 MPa)
Poisson's ratio	0.25

Foam is a material characterized by low cost and low weight, which reduces the weight of the structure. It also has good fire and thermal resistance as well as excellent impact properties. Because of these properties, it acts very well as an insulation material. There are many types of foams, such as polystyrene, polyethylene and polyurethane foam. These types vary in both properties and cost. Because of the lower cost, expanded polystyrene (EPS) foam was selected for use as a core for CSIP. Table 2 describes the properties of the EPS foam, as provided by the manufacturer [18].

Table 3.
Dimensions of CSIP floor panels

T	0.12 in. (3.04 mm)
C	5.5 in. (140 mm)
D	5.74 in. (146.08 mm)
B	48 in. (1219.2 mm)
L	96 in. (2438.4 mm)

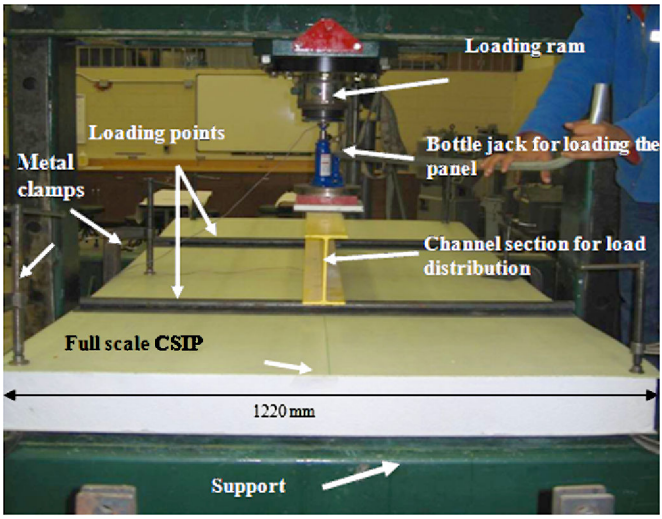

Figure 2. Experimental setup for the floor test according to ASTM-E-72-05. This figure is published in color in the online version.

The glass–PP facesheets are bonded to the EPS core using a hot-melt thermoplastic spray adhesive. This method of manufacturing is fast and less labor intensive than manufacturing of traditional SIPs. Typical dimensions of the OSB SIPs currently used in the modular buildings are 4 ft × 8 ft (1219.2 mm × 2438.4 mm) [19]. Thus, the overall dimensions (length and width) of the CSIP panels were maintained the same (Table 3). To insure quality of processing, CSIPs floor panels were manufactured at a casting and molding facility.

4. Experimental Work

The experimental testing was performed according to the ASTM E-72-05 standard [20]. This standard deals with testing panels for structural building applications. The proposed panels were tested using a four-point bend setup as shown in Fig. 2. The load was applied through a bottle jack of capacity 6 metric tons distributed over the panel using a spreader I-beam as shown in Fig. 2. The deflection at the mid-span was recorded using a linear variable displacement transducer (LVDT)

with a capacity of measuring deflection up to 150 mm. Strain gages with gage factor of 2.085 were attached at the geometric center on the top and bottom facesheets of the panels. The LVDT, load cell, and strain gages were connected to the data acquisition machine, which in turn recorded the data using Strain Smart software. Two full scale specimens of 4 ft × 8 ft (1219.2 mm × 2438.4 mm) were tested on the setup mentioned above.

4.1. Experimental Results and Discussion

At a load of 1.8 kip (8 kN), the panel failed by localized debonding between the core and top facesheets in the maximum flexural zone in compression (Fig. 3). This mode of failure is known as wrinkling of the facesheet in compression, which was caused by a sudden local buckling of the facesheets. The main reason for the facesheet/core debonding is the much lower properties of the core compared to that of the facesheets. Further, the softness of the core could not maintain the curvature due to the out-of-plane debonding attributed to very soft core (referring to EPS foam). Therefore, the flexural failure of the CSIP floor panel is controlled by limited strain at the facesheet/core interface. This strain was the same for both panels. In the case of the rigid core, the common mode of failure is the rupture of the facesheet in tension in the maximum flexural zone (Fig. 4). This was the same for a research conducted by the authors on a sandwich panel with rigid core [7]. Figure 5 shows schematic diagrams for the failure in the flexural zone for sandwich panels made of soft and rigid cores.

As seen from Fig. 6, the load–deflection curve for the two panels is similar. The load *versus* deflection response was seen to be linear. The corresponding deflection at the peak load was 2.08 in. (53 mm). Loading was then stopped (at 1.8 kip (8 kN)) and panels were unloaded. A permanent set of 0.16 in. (4 mm) was measured for both the panels upon unloading.

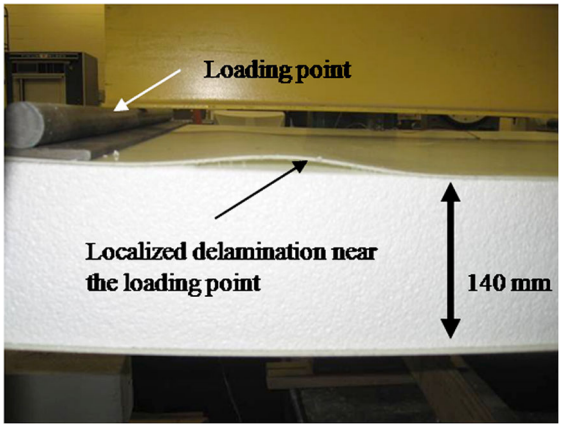

Figure 3. Typical failure of the CSIP floor panels at the peak load. This figure is published in color in the online version.

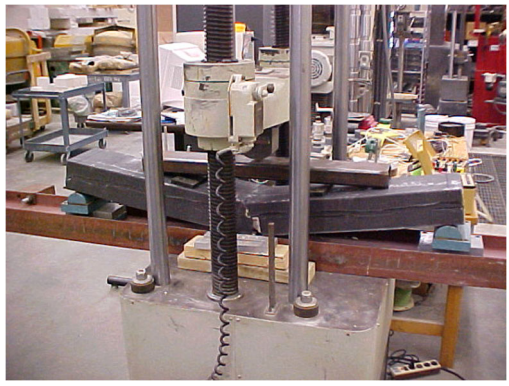

Figure 4. Typical failure of the sandwich panel with rigid core in the maximum flexural zone [7]. This figure is published in color in the online version.

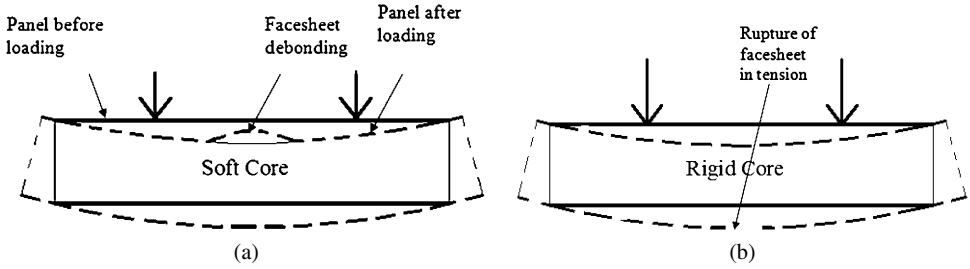

Figure 5. Flexural failure of sandwich panels.

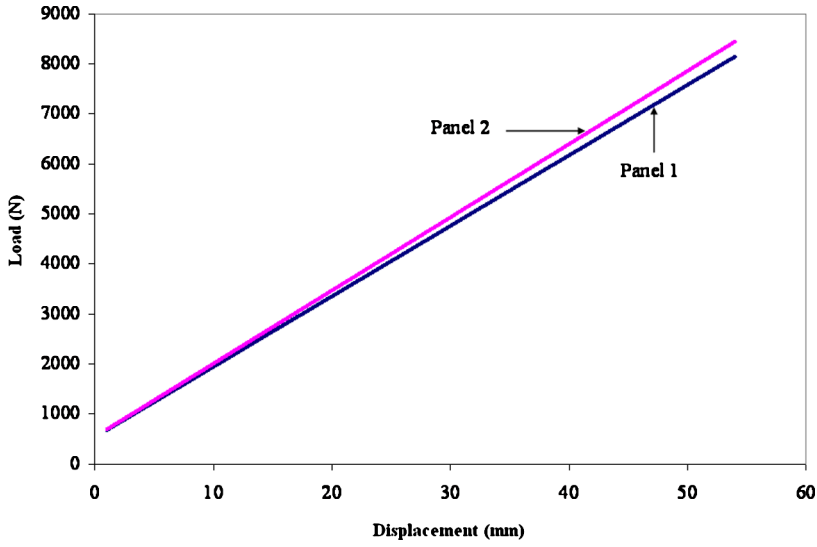

Figure 6. Load *versus* mid-span deflection of the CSIP floor panels. This figure is published in color in the online version.

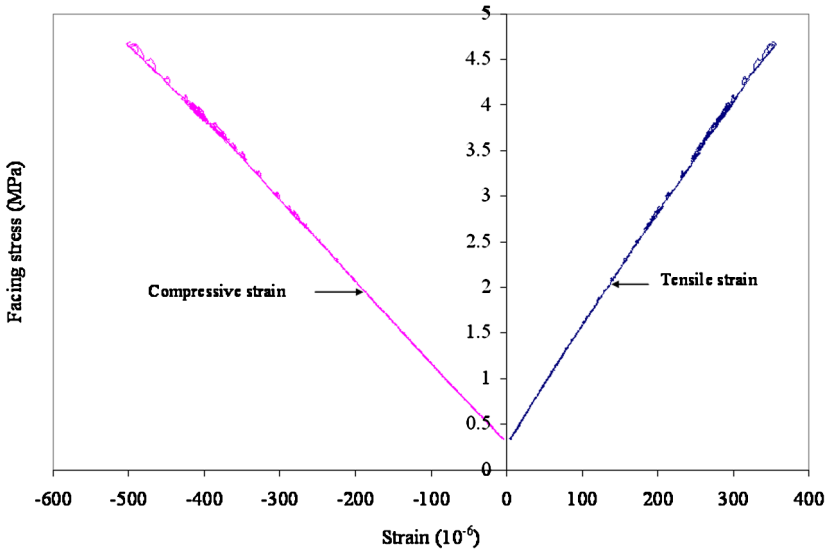

Figure 7. Load *versus* strain for CSIPs. This figure is published in color in the online version.

The applied load *versus* lateral strain is plotted in Fig. 7. As seen for the load–deflection curve, a high degree of repeatability was observed in the strains produced in the two panels. A linear relationship is observed between the load and strain until failure. This is refers to the elastic behavior of the CSIP floor panels. It can be noted from Fig. 7 that the compressive strain produced in the top facesheet at each load level was a little higher than that produced in the tensile facesheet. The top and bottom facesheets exhibit unequal strains because the foam core is compressible. As the foam cells collapsed under compression loading, the foam cells were engaged in tension along with the facesheet. Due to this, the compressive strains were observed to be higher than the tensile strains during testing. The compression of the foam cells caused shifting of the neutral axis creating unequal strains in top and bottom facesheets [21].

5. Analytical Work

In general, there are two main criteria controlling the design of the sandwich panel: strength and deflection. As observed in the experiment, CSIP floor panels failed by facesheet/core debonding in the compression side which is related to strength. Deflection prior to debonding is also another issue that needs to be checked with the building code limit. Therefore, in the theoretical analysis presented in this section, models for stresses at debonding and deflection were developed. Stresses at facesheet/core debonding were modeled based on the Winkler foundation model whereas deflection was calculated based on the effective panel thickness.

5.1. Stresses at the Facesheet/Core Debonding

During loading of a sandwich floor panel, two types of stresses are developed at the facesheet in the compression side: the first is a tensile out-of-plane stress at facesheet/core interface 'σ_z' while the other is a compressive critical wrinkling stress in the facesheet of the deboned part 'σ_{cr}' (Fig. 8). The debonding occurs when the tensile stress at the facesheet/core interface exceeds the tensile strength of the core material (e.g., EPS foam). It is a common mode of failure of sandwich panels, leading to reduced panel stiffness. As far as the wrinkling or debonding is concerned, there are three main categories known as: Case I: rigid base (single-sided); Case II: antisymmetrical; and Case III: symmetrical (Fig. 9). Case I occurs in the case of sandwich panel under pure bending moment or wall panel under eccentric loading in which the debonding is likely to occur at one side only. Case II and Case III occur in the case of wall panels subjected to in-plane axial load. Detail explanation for the three cases is provided in Allen [12]. Since CSIP floor panels were subjected to out-of-plane loading, Case I was the mode of failure as demonstrated in the experiment.

The glass–PP facesheets under compression can be modeled as a strut or beam supported by an elastic foundation represented by the EPS foam core. In other words, CSIPs wrinkling can be modeled as a Winkler foundation. In the analysis of the behavior of a long strut or beam supported by a continuous elastic medium; the medium can be replaced by a set of closed-spaced springs (Fig. 10); this phenomenon is normally known as Winkler hypothesis, and the facesheet in this case is called Winkler beam while the core is known as Winkler foundation. For a beam

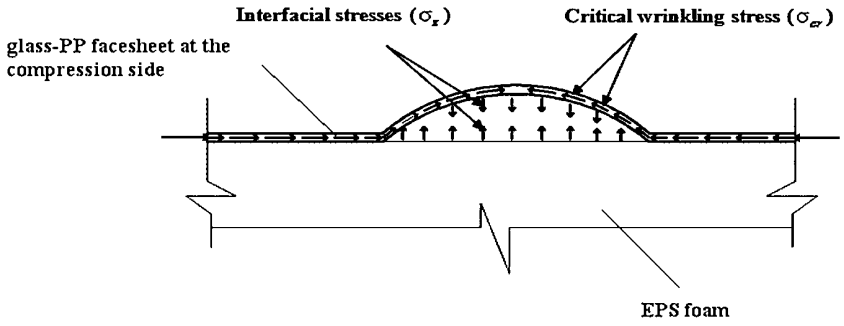

Figure 8. Types of stresses developed at the compressive side of CSIP floor panel at debonding.

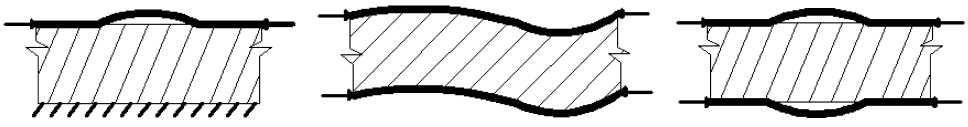

Figure 9. Types of wrinkling.

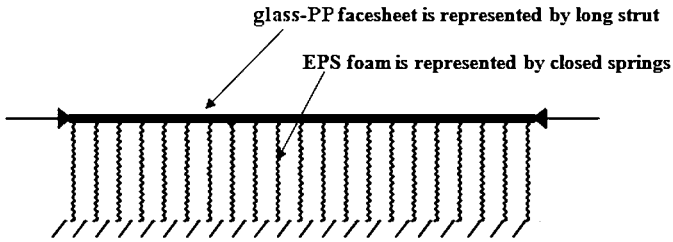

Figure 10. Winkler foundation model for CSIP.

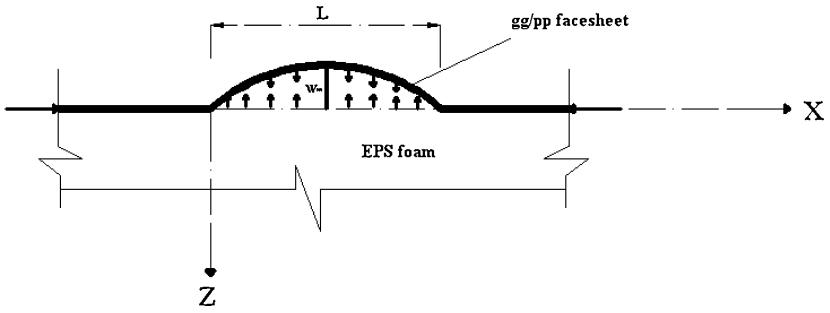

Figure 11. Half-wavelength of the debonded facesheet in compression.

supported by a Winkler foundation, the governing differential equation of the beam is given as:

$$D_{\mathrm{f}}\frac{\mathrm{d}^4 w}{\mathrm{d}x^4} + P\frac{\mathrm{d}^2 w}{\mathrm{d}x^2} + b\sigma_z = 0, \tag{1}$$

where D_{f} the flexural stiffness of the beam (facesheet), P is axial load developed in the facesheet due to loading, w is the displacement of the debonded part in z-direction. σ_z is the interfacial tensile stress at facesheet/core interface, and b is the width of the facesheet.

5.1.1. Interfacial Tensile Stress (σ_{z})

Assume the springs' (foundation) stiffness is represented by a coefficient k. This coefficient represents the force needed to displace the springs in a unit area of the xy-plane through a unit displacement in the z-direction. Suppose this strut buckle into sinusoidal waves with half-wavelength of l which is equal to the deboned length (Fig. 11), the displacement of the buckled portion in the z-direction can be expressed as:

$$w(x) = w_{\mathrm{m}} \sin\frac{\pi x}{l}, \tag{2}$$

where w_{m} is the maximum displacement of the deboned part (i.e., at $l/2$). The Winkler beam model assumes that displacements of facesheet in compression are symmetrical about the center line of the core while displacements the facesheet in tension are negligible. It should be mentioned that, as demonstrated by earlier

studies [12, 23, 24], the half-wavelength (l) of the debonded part is always of the same order as the thickness of the core. A similar observation was made in this study, when experimental testing demonstrated that the debonded part is almost equal to the core thickness (see Fig. 3). As shown in Fig. 11, the corresponding out-of-plane stress (interfacial tensile stress) that is required to displace this portion of facesheet is given by:

$$\sigma_z = k \cdot w. \tag{3}$$

From equations (2) and (3), we get:

$$\sigma_z = k w_{\mathrm{m}} \sin \frac{\pi x}{l}. \tag{4}$$

Several investigations have been conducted to model the foundation stiffness k (Sleight and Wang [25]; Niu and Talreja [26]). However, we are proposing in this study the stiffness foundation suggested by Allen [12], which includes the effect of the half-wavelength of the debonded facesheet as well as the wrinkling type unlike the previous models. It is also used for isotropic core (i.e., EPS foam). The general equation for k to represent the three cases of wrinkling can be expressed as:

$$k = \frac{E_{\mathrm{c}}}{c} \theta^2 f(\theta). \tag{5}$$

From equations (4) and (5), the tensile stress at the facesheet/core interface for a given displacement (w_{m}) and half-wavelength (l) for the debonded facesheet can be given as:

$$\sigma_z = \frac{E_{\mathrm{c}}}{c} \theta^2 f(\theta) w_{\mathrm{m}} \sin \frac{\pi x}{l}. \tag{6}$$

For Case I, referring to the control failure case in this study, $f(\theta)$ can be given by:

$$f(\theta) = \frac{2}{\theta} \frac{(3 - \upsilon_c) \sinh\theta \cosh\theta + (1 + \upsilon_c)\theta}{(1 + \upsilon_c)(3 - \upsilon_c)^2 \sinh^2\theta - (1 + \upsilon_c)^3 \theta^2}. \tag{7}$$

The debonding occurs when this stress exceeds the tensile stress of the core material. Further, and as noticed from equation (6), the interfacial stress is independent of the facesheet properties whereas it depends only on the core properties as well as core thickness. θ is a function of the core thickness and half-wavelength of l and is given by $\frac{\pi c}{l}$. $f(\theta)$ is a function of core Poisson's ratio and θ, and it has a different equation for each case of wrinkling.

5.1.2. Critical Wrinkling Stress in the Facesheet (σ_{cr})

The second stress that is associated with the debonding is the critical wrinkling stress in the facesheet in compression (σ_{cr}). This is a compressive in-plane stress developed in the facesheet due to loading. To model this stress (σ_{cr}), the analysis is based also on the Winkler beam model presented above. Substitution of $w(x)$ from equation (2) and (σ_z) from equation (6) into equation (1) and rearranging the equation, yields:

$$P \frac{\pi^2}{l^2} = b \frac{E_{\mathrm{c}}}{c} \theta^2 f(\theta) + D_{\mathrm{f}} \frac{\pi^4}{l^4}. \tag{8}$$

For orthotropic facesheets, referring to glass–PP facesheet laminates, D_f is given by

$$D_f = \frac{bE_f t^3}{12}\left(1 - \upsilon_{xy}^2\right), \tag{9}$$

where υ_{xy} is the Poisson's ratio of the facesheet in the xy-plane. This will consider the through thickness anisotropy effect due to the orthotropic facesheets [27]. Dividing equation (8) by bt and substituting of D_f, $\frac{\pi}{l} = \frac{\theta}{c}$, recognizing that the wrinkling compressive stress in the facesheet (σ_{cr}) is given as P/bt, this yields:

$$\sigma_{cr} = \frac{E_c}{t} cf(\theta) + \frac{E_f}{12}\left(\frac{\theta}{c}\right)^2 t^2\left(1 - \upsilon_{xy}^2\right). \tag{10}$$

As seen in equation (10), the wrinkling stress (σ_{cr}) is a function of the properties and thicknesses of facesheet and core unlike the interfacial tensile stress (σ_z) which is independent of the facesheet properties and mainly depends on the core material.

Several investigations were conducted to predict the critical wrinkling stress for all wrinkling cases. Most of these studies have led to empirical formulas. All the formulas take the following form for sandwich panels with solid cores (such as EPS foam):

$$\sigma_{cr} = \beta(E_f E_c G_c)^{1/3}. \tag{11}$$

The value of the constantβ in equation (11) has been suggested by various investigators (0.79 and 0.63 by Gough *et al.* [14], 0.76 by Cox and Riddell [28], 0.91 and 0.5 by Hoff and Mautner [15], 0.825 by Plantema [29]). From this discussion, it can be seen that there are different approaches regarding the calculation of the wrinkling stress in the compressive facesheet. Further, most of these studies considered only isotropic facesheets when the sandwich panels used to have isotropic facesheets made of metal. In this study, the model derived for the wrinkling stress is taking into consideration the orthotropic facesheets and the solid core.

Based on the critical wrinkling strength, the flexural strength of the floor panel can be calculated too. The flexural strength of the sandwich panels is developed due to the internal force couple in the facesheets. The core works as a separator between the two forces, as shown in Fig. 12, and carries the shear stresses [7]. C and T are the compressive and tensile forces carried by the facesheets, respectively. These

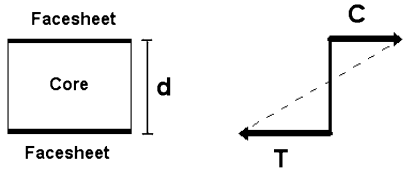

Figure 12. Force diagram for a sandwich panel cross section.

forces are approximately equal in magnitude. Thus, the flexural strength can be expressed as:

$$M_n = T \cdot d = C \cdot d. \tag{12}$$

The forces in the facesheets are determined as follows:

$$T = C = A \cdot \sigma_{cr}, \tag{13}$$

where A is the area for each facesheet and σ_{cr} is the critical wrinkling stress in the facesheets which can be determined from equation (11)

$$T = C = b \cdot t_f \cdot \sigma_{cr}. \tag{14}$$

Therefore, the nominal flexural strength for sandwich panel is given by:

$$M_n = b \cdot t_f \cdot \sigma_{cr} \cdot d. \tag{15}$$

5.2. Deflection

The total central deflection of a sandwich panel under out-of-plane loading is composed of bending deflection and shear deflection. The general formula for the deflection of a sandwich panel under out-of-plane loading is given by:

$$\Delta = \frac{k_b P L^3}{D} + \frac{k_s P L}{U}. \tag{16}$$

In the above equation, the first term on the right-hand side of the equation is the deflection due to bending, and the second term is the deflection due to shear (Fig. 13): k_b and k_s are the bending and shear deflections coefficients, respectively. The values of both k_b and k_s depend on the loading and boundary conditions. For the CSIP floor panels tested in this study, (two-point load, one-fourth span with simply supported boundary conditions), k_b and k_s are 11/768 and 1/8, respectively. For the sake for brevity, the derivation of k_b and k_s is not included in this paper and the basis for deriving them can be found elsewhere [12]. D and U are flexural and shear rigidities of the sandwich panel, respectively. According to ASTM C-393

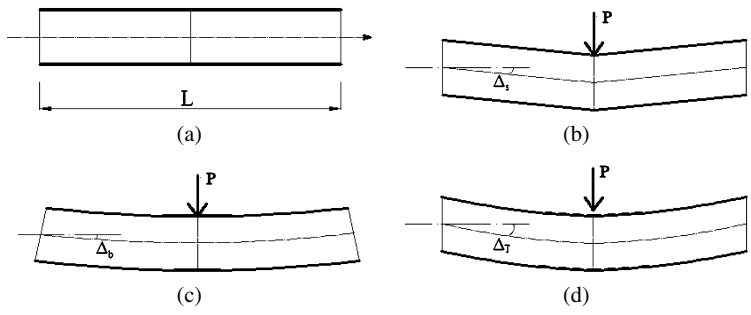

Figure 13. Deflection of sandwich panel.

[22], D and U can be determined as follows:

$$D = \frac{E_{\text{face}}(d^3 - c^3)b}{12}, \tag{17}$$

$$U = \frac{G_{\text{core}}(d + c)^2 b}{4c}. \tag{18}$$

Equation (17) assumes only isotropic facesheets while to consider orthotropic facesheets such as glass–PP used for CSIP, equation (2) should be multiplied by $(1 - \upsilon_{xy}^2)$ where υ_{xy} is the in-plane Poisson's ratio of the orthotropic facesheets in the xy-plane. Therefore, equation (17) becomes:

$$D = E_{\text{f}} I = \frac{E_{\text{f}}(d^3 - c^3)b}{12}\left(1 - \upsilon_{xy}^2\right). \tag{19}$$

It is generally recognized that the ordinary theory of bending and resulting deflection can be applied to a homogenous panel (that is, a panel that is made from one material). For a sandwich panel, the behavior is different and this can be demonstrated by considering two extreme cases. First, when the core is rigid in shear, the sandwich panel is subjected to the same argument as those applied to a homogenous panel (except for the difference in the flexural rigidity) and the deflections are expected to be small. Second, when the core is weak in shear, the faces act as two independents plates and the resulting deflections are expected to be much higher than the first case. It was demonstrated by Allen [12], that the parameter λ represents the transition from one extreme to the other (known also as effective depth coefficient), varying from $(-t/c)$ when the core is weak to $(+1)$ when the core is rigid in shear. Thus, an empirical formula was developed by Allen [12] to define the effective thickness of a sandwich panel which varies from $2t$ $(G = 0)$ to d $(G = \infty)$:

$$d_{\text{eff.}} = t\left(1 + \frac{c}{d}\right) + \frac{c^2}{d}\lambda. \tag{20}$$

6. Validation of the Experimental Results

6.1. Stresses at Debonding

6.1.1. Interfacial Tensile Stress (σ_{z})

As shown in Fig. 14, the half-wavelength is almost equal to the core thickness (140 mm) and the maximum out-of-plane displacement (w_{m}) of the debonded facesheet is almost 10 mm for both panels. Therefore, the function θ can be determined as follows:

$$\theta = \frac{\pi c}{l} = \frac{\pi(140)}{140} = 3.14.$$

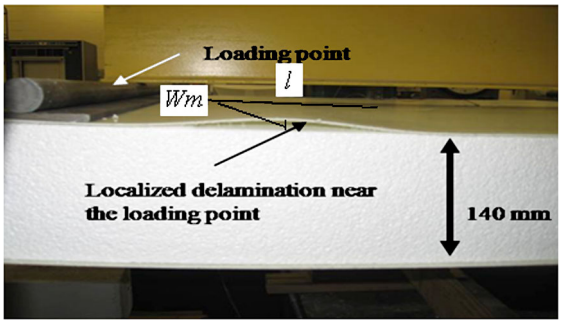

Figure 14. Failure of CSIP floor panel under out-of-plane loading. This figure is published in color in the online version.

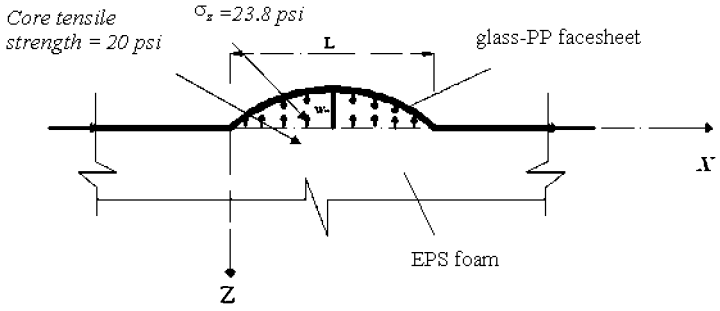

Figure 15. Out-of-plane stress of CSIP floor panel.

As observed in the experimental; w_{m} (10 mm) represents 7% of the core thickness, $c = l$, $\sin\frac{\pi x}{l} =$ unity since the stress is calculated at the middle. Accordingly, and for the design purpose, equation (6) can be rewritten as:

$$\sigma_z = 0.07\pi^2 f(\theta) E_{\mathrm{c}}. \tag{21}$$

$f(\theta)$ is determined according to equation (7):

$$f(\theta) = \frac{2}{3.14}\frac{(3-0.25)\sinh(3.14)\cosh(3.14) + (1+0.25)(3.14)}{(1+0.25)(3-0.25)^2\sinh^2(3.14) - (1+0.25)^3(3.14)^2} = 0.191.$$

Thus, the interfacial out-of-plane stress can then be determined from equation (14) as follows:

$$\sigma_z = 0.07\pi^2(0.191)(1.2) = 0.16\ \mathrm{MPa} = 23.8\ \mathrm{psi}.$$

As seen from Table 2, the maximum tensile strength of the EPS core is 20 psi. As previously mentioned, the debonding occurs when the interfacial stress exceeds the tensile strength of the core material. As demonstrated from the model, the out-of-plane stress (23.8 psi) has exceeded the tensile strength of the core material (20 psi) thereby initiating debonding failure as observed. Figure 15 illustrates these values.

6.1.2. Critical Wrinkling Stress (σ_{cr})

As shown in the Fig. 7, the compression strain at the debonding is 0.0005. This strain results from an experimental wrinkling stress of:

$$\begin{aligned} \sigma_{\text{cr Exp.}} &= \varepsilon_{\text{exp.}} \cdot E_{\text{f}}, \\ \sigma_{\text{cr Exp.}} &= 0.0005(15\,169) = 7.58 \text{ MPa}. \end{aligned} \tag{22}$$

Since Case I is the control case for floor and walls panels, $f(\theta)$ is determined according to equation (7):

$$f(\theta) = \frac{2}{3.14} \frac{(3-0.25)\sinh(3.14)\cosh(3.14) + (1+0.25)(3.14)}{(1+0.25)(3-0.25)^2\sinh^2(3.14) - (1+0.25)^3(3.14)^2} = 0.191$$

and θ can be determined as follows:

$$\theta = \frac{\pi c}{l} = \frac{\pi \times 140}{140} = 3.14.$$

Accordingly, the theoretical wrinkling stress can be calculated using equation (10) as follows:

$$\begin{aligned} \sigma_{\text{cr}} &= \frac{E_{\text{c}}}{t} c f(\theta) + \frac{E_{\text{f}}}{12}\left(\frac{\theta}{c}\right)^2 t^2\left(1-\upsilon_{xy}^2\right) \\ &= \frac{1.2}{3.04}(140)(0.191) + \frac{15\,169}{12}\left(\frac{3.14}{140}\right)^2 (3.04)^2(1-0.11^2) = 16.43 \text{ MPa}. \end{aligned}$$

Comparing the experimental value of the wrinkling stress (7.58 MPa) with the theoretical value predicted by the proposed model (16.43 MPa), it can be noticed that the experimental value is almost one-half of the theoretical one. This was common for most of the previous works conducted on wrinkling stress (for example, in Hoff and Mautner [15], the theoretical constant went from 0.91 to 0.5 to fit the experimental results). Thus, these studies have proposed an empirical formula to correlate with the experiments.

In this case, the core has much lower mechanical properties compared to that of the facesheets in which the ratio of facesheet modulus to that of the core is the highest ratio that been used for a sandwich panel to date ($E_{\text{f}}/E_{\text{c}} = 12\,500$ in this study *versus* 1000 for other studies reported in the literature). It can be noticed that the critical wrinkling stress of the wall (i.e., 7.5 MPa) can be predicted using equation (11) with $\beta = 0.25$. Accordingly, to fit with the experimental results, the following empirical formula is, therefore, proposed to predict the wrinkling stress of the CSIPs taking into consideration the orthotropic facesheets:

$$\sigma_{\text{cr}} = 0.25(E_{\text{f}}E_{\text{c}}G_{\text{c}})^{1/3}\left(1-\upsilon_{xy}^2\right). \tag{23}$$

By comparing the proposed constant (0.25) with the other constants previously proposed for sandwich structures, it can be noticed this constant is smaller than the ones that have been used before. The main reasons for that include the orthotropic facesheet used in the study and the high moduli ratio of the facesheet and core.

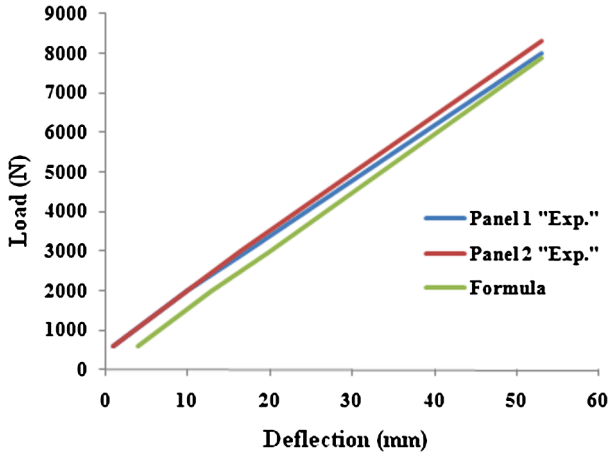

Figure 16. Experimental *versus* expected deflection for CSIPs floor panels. This figure is published in color in the online version.

6.2. *Deflection*

$d_{\text{eff.}}$ should be used instead of d in equations (17) and (18) when determining the flexural and shear rigidities. Effective depth coefficient (λ) is determined experimentally based on the deflection. The procedure for calculating λ is as follows; first, the effective sandwich depth ($d_{\text{eff.}}$) is determined using equation (19) by trial and Δ is taken from experiment (i.e., 53 mm). Secondly, using $d_{\text{eff.}}$ and the actual sandwich thicknesses, λ is determined from equation (19). A detail procedure for calculating λ is provided in the Appendix. In this study, λ was determined for CSIPs floor panel based on the experimental deflection and was found to be 0.31. Thus, equation (19) can be rewritten as follows:

$$d_{\text{eff.}} = t\left(1 + \frac{c}{d}\right) + 0.31\frac{c^2}{d}. \tag{24}$$

Figure 16 shows a comparison of the experimental deflection and theoretical deflection throughout the loading of the panels until failure. The theoretical deflections were calculated using the nominal thickness ($d_{\text{eff.}}$) obtained from equation (24) with λ of 0.31.

7. Conclusions

A new type of composite structural insulated panels (CSIPs) was presented for structural floor applications to replace traditional SIPs that are made using wood-based facing. The behavior of these panels was investigated under full scale out-of-plane loading. Theoretical models were developed for stresses at facesheet/core debonding and deflection. The experimental results were validated using these models and were in good agreement. The main conclusions of this study

are:

1. The general model of failure of CSIPs floor panelling was facesheet/core debonding at the compression side with a natural half-wavelength equal to the core thickness ($l = c$). The main reason for this mode is that the out-of-plane tensile stress at the facesheet/core interface exceeded the tensile strength of the core.
2. The behaviors of both panels were linear until debonding as can be seen from the load *versus* deflection and load *versus* strain curves.
3. A theoretical model for the interfacial stress for a CSIP floor member was developed based on the Winkler foundation model and validated using the experimental results. The results proved that the predicted interfacial stress is higher than core tensile strength and so debonding was the general mode of failure. This validates the criteria that the interfacial stress is independent of loading and boundary conditions and depends only on the core properties.
4. The proposed theoretical model for the critical wrinkling stress based on the Winkler foundation model less conservatively predicted the actual wrinkling stress. Accordingly, an empirical formula was proposed to predict the critical wrinkling stress at the debonding for CSIP floor panels considering the orthotropic facesheets. Further, a formula for the nominal flexural capacity for CSIP floor panels was developed.
5. An effective thickness formula for CSIPs floor member was developed to be used when calculating the deflection. The effective thickness is less than the nominal thickness since the facesheet and core used for producing CSIP have a very high moduli ratio ($E_f/E_c = 12\,500$).

Acknowledgements

The authors gratefully acknowledge funding and support provided by National Science Foundation (NSF) for this research project (CMMI-825938). They also would like to thank Dr Amol Vaidya for his help in the experimental results.

References

1. D. Zenkert, *An Introduction to Sandwich Construction*. Engineering Materials Advisory Service Ltd, West Midlands, United Kingdom (1995).
2. M. Mousa, Optimization of structural panels for cost-effective panelized construction, *MS Thesis*, CCEE Department, University of Alabama at Birmingham, USA (2007).
3. A. Khotpal, Structural characterization of hybrid fiber reinforced polymer (FRP)-autoclaved aerated concrete (AAC) panels, *MS Thesis*, C.C.E.E. Department, University of Alabama at Birmingham, USA (2004).

4. K. Shelar, Manufacturing and design methodology of hybrid fiber reinforced polymer (FRP)-autoclaved aerated concrete (AAC) panels and its response under low velocity impact, *MS Thesis*, C.C.E.E. Department, University of Alabama at Birmingham, USA (2006).
5. N. Uddin and H. Fouad, Structural behavior of FRP reinforced polymer-autoclaved aerated concrete panels, *ACI Struct. J.* **104**, 722–730 (2007).
6. S. Vaidya, Lightweight composites for modular panelized construction, *PhD Dissertation*, C.C.E.E. Department, University of Alabama at Birmingham, USA (2009).
7. M. Mousa and N. Uddin, Experimental and analytical study of carbon fiber-reinforced polymer (FRP)/autoclaved aerated concrete (AAC) sandwich panels, *J. Engng Struct.* **31**, 2337–2344 (2009).
8. S. Chevali, Flexural creep of long fiber thermoplastic composites: effect of constituents and external variable on non-linear viscoelasticity, *PhD Dissertation*, M. E. Department, University of Alabama at Birmingham, USA (2009).
9. I. M. Daniel, E. E. Gdoutos, K. A. Wang and J. L. Abot, Failure modes of composites sandwich beams, *Intl J. Damage Mech.* **11**, 309–334 (2002).
10. E. E. Gdoutos, I. M. Daniel and K.-A. Wang, Compression facing wrinkling of composite sandwich structures, *J. Mech. Mater.* **35**, 511–522 (2003).
11. G. A. Kardomateas, Global buckling of wide sandwich panels with orthotropic phases, in: *Proc. 7th Intl Conf. Sandwich Structures*, Aalborg University, Denmark (2005).
12. H. G. Allen, *Analysis and Design of Structural Sandwich Panels*. Pergamon Press Ltd., London, UK (1969).
13. G. G. Galletti, C. Vinquist and O. S. Es-said, Theoretical design and analysis of a honeycomb panel sandwich structure loaded in pure bending, *J. Engng Failure Anal.* **15**, 555–562 (2007).
14. G. S. Gough, C. F. Elam and N. D. de Bruyne, The stabilization of a thin sheet by a continuous supporting medium, *J. Royal Aeronaut. Soc.* **44**, 12–43 (1940).
15. N. J. Hoff and S. F. Mautner, The buckling of sandwich-type panels, *J. Aeronaut. Sci.* **12**, 285–297 (1945).
16. T. Hartness, G. Husman, J. Koening and J. Dyksterhouse, The characterization of low cost fiber reinforced thermoplastic composites produced by DRIFT process, *Composites: Part A* **32**, 1155–1160 (2001).
17. Company literature, Crane Composites, Inc., 23525 W Eames, Channahon, IL 60410, USA.
18. Company literature, Universal Packaging, Inc., 2216 Greenspring Drive Lutherville, MD 21093, USA.
19. M. Morley, *Building with Structural Insulated Panels*. The Taunton Press, Newtown, CT, USA (2000).
20. *Annual Book of ASTM Standards E-72-05*, Standard test method of conducting strength tests of panels for building construction, 100 Barr Harbor Drive, West Conshohocken, PA 19428-2959, USA (2005).
21. H. Alwin, Development of a method to analyze structural insulated panels under transverse loading, *Master Thesis*, Washington State University, USA (2002).
22. *Annual Book of ASTM Standards C393-00*, Standard test method for flexural properties of sandwich construction, 100 Barr Harbor Drive, West Conshohocken, PA 19428-2959, USA (2000).
23. W. K. Vonach and F. G. Rammerstorfer, Wrinkling of thick orthotropic sandwich plates under general loading conditions, *Archive Appl. Mech.* **70**, 338–348 (2000).
24. T. Southward, G. D. Mallinson, K. Jayaraman and D. Horrigan, Buckling of disbonds in honeycomb-core sandwich beams, *J. Sandwich Struct. Mater.* **10**, 195–216 (2008).

25. D. W. Sleight and J. T. Wang, *Buckling Analysis of Debonded Sandwich Panel under Compression*, NASA Tech Memorandum 4701, USA (1995).
26. K. Niu and R. Talreja, Buckling of a thin face layer on Winkler foundation with debonds, *J. Sandwich Struct. Mater.* **1**, 259–278 (1999).
27. R. P. Ley, W. Lin and U. Mbanefo, Facesheet wrinkling in sandwich structures, NASA/CR-1999-208994 (1999).
28. H. L. Cox and J. R. Riddell, Sandwich construction and core materials III: instability of sandwich struts and beams, ARC Technical Report R and M 2125 (1945).
29. F. J. Plantema, *Sandwich Construction.* John Wiley, New York, USA (1966).

Appendix: λ Calculations for CSIPs Floor Panels

Data

The experimental deflection = 2.09 in. (53 mm)

$L = 8$ ft (2438.4 mm), $b = 4$ ft (1219.2 mm), $c = 5.5$ in. (139.7 mm), $t = 0.12$ in. (3.04 mm), $d = 5.74$ in. (145.78 mm), $P = 1.8$ kips (8000 N)

$k_b = 11/768$

$k_s = 1/8$

Theoretical deflection

To obtain λ, we have to assume it is equal to 1 and then get the theoretical deflection according to the following equation:

$$\Delta = \frac{k_b P L^3}{D} + \frac{k_s P L}{U},$$

$$D = \frac{E_{face}(d^3 - c^3)b}{12} = \frac{15\,169(145.84^3 - 139.7^3)1219.2}{12} = 5.78 \times 10^{10}\ \text{N mm}^2,$$

$$U = \frac{G(d+c)^2 b}{4c} = \frac{2.05(145.8 + 139.7)^2 1219.2}{4 \times 139.7} = 11.9 \times 10^4\ \text{N},$$

$$\Delta = \frac{11 \times 8000 \times 2438.4^3}{768 \times 5.78 \times 10^{10}} + \frac{1 \times 8000 \times 2438.4}{8 \times 11.9 \times 10^4} = 9.9\ \text{mm},$$

i.e., using the actual panel thickness, the deflection is 9.9 mm which is much lower than the experimental deflection (53 mm) due to core softness. After trials, it was found that the nominal thickness (d_{nom}) that can provide the experimental deflection is 1.88 in. (47.68 mm). Accordingly, λ can be determined as follows:

$$47.68 = 3.04\left(1 + \frac{139.7}{145.84}\right) + \frac{139.7^2}{145.84}\lambda.$$

The above equation results in a value for $\lambda = 0.31$.